

A new method for estimating widths, velocities, and source location of halo CMEs.

G. Michalek

Astronomical Observatory of Jagiellonian University

michalek@oa.uj.edu.pl

and

N. Gopalswamy

Center for Solar and Space Weather, Catholic University of America

and

S. Yashiro

Center for Solar and Space Weather, Catholic University of America

ABSTRACT

It is well known that coronagraphic observations of halo coronal mass ejections (CMEs) are subject to projection effects. Viewing in the plane of the sky does not allow us to determine the crucial parameters defining geoeffectiveness of CMEs, such as the space speed, width or source location. Assuming that halo CMEs have constant velocities, are symmetric and propagate with constant angular widths, at least in their early phase, we have developed a technique which allows to obtain the required parameters. This technique requires measurements of sky-plane speeds and the moments of the first appearance of the halo CMEs above opposite limbs. We apply this technique to obtain the parameters of all the halo CMEs observed by the Solar and Heliospheric Observatory (SOHO) mission's Large Angle and Spectrometric Coronagraph (LASCO) until the end of 2000. We also present a statistical summary of these derived parameters of the halo CMEs.

Subject headings: Coronal mass ejections—solar physics—space weather

1. Introduction

Space weather is significantly controlled by coronal mass ejections (CMEs) which can affect the Earth in different ways. CMEs originating from regions close to the central meridian of the Sun and directed toward the Earth are of immediate concern because they are likely to be geoeffective. In coronagraphic observations, halo CMEs appear as enhancement surrounding the entire occulting disk (Howard et al. 1982). Halo CMEs are routinely recorded by the highly sensitive SOHO/LASCO coronagraphs. In spite of the large advantage over previous instruments, the SOHO/LASCO observations are still affected by projection effects because of the nature of Thomson scattering (Gopalswamy et al. 2000b). Viewing in the plane of the sky does not allow us to determine the crucial parameters (space speed, width, and source location) defining geoeffectiveness of CMEs. Prediction of the arrival of CME in the vicinity of Earth is critically important in space weather investigations. Based on interplanetary CMEs detected by Wind and the corresponding CMEs remote-sensed by SOHO, Gopalswamy et al. (2000a; 2002b) developed and improved an empirical model to predict the arrival of CMEs at 1AU. The critical input to this model is the initial CME speed. Better prediction could be achieved if true initial velocities are used instead projected velocities determined from LASCO observations. Attempts have been made to estimate the projection effects based on the location of the solar source by employing ad hoc assumptions on the parameters such as the CME width (Sheeley et al. 1999, Leblanc et al., 2001). In the present paper we attempt to determine the space speed, width or source location using a different technique by assuming that the CME is shaped like an ice-cream cone. The method is based on the following assumptions: (i) the halo CMEs at least in the very early phase have constant velocities, (ii) they are symmetric, and (iii) propagate with constant angular widths. The required inputs are the sky plane speeds along two opposite directions and the times of first appearance above the limb in those two directions. We apply this technique to all the halo CMEs observed by SOHO/LASCO until the end of 2000. We compare the parameters obtained from this technique with those listed in the SOHO/LASCO CME catalog.

2. The cone model of CME

In the projection on the sky most of the CMEs (especially limb events) observed by the LASCO coronagraph look like cone shape blobs as schematically illustrated in Figure 1. They maintain this shape during expansion through the C2 and C3 fields of view. The observed angular widths, for many limb events, remain nearly constant as a function of height (see, e.g., Webb et al. 1997). Most of them propagate with constant radial frontal speed but many slow CMEs gradually accelerate whereas many fast CMEs decelerate (St.

Cyr et al., 2000; Sheeley et al., 1999; Gopalswamy et al., 2001; Yashiro et al. 2002(conference presentation)). Assuming that the halo CME propagate with a constant velocity and angular width we can reproduce it by the cone model with four free parameters: velocity, angular width, orientation of the central axis of the CME, and the distance of source location from the central meridian measured in the plane of the sky. These assumptions should be true at least in the beginning phase of the CME expansion. Therefore we assume that bulk velocity of the CME is directed radially and isotropic. Similar cone models have been used before, e.g., by Howard et al. (1982), Fisher and Munro (1984), and recently by Zhao et al. (2002). In the Fig. 1. we show schematically basic properties of the CME model. In the projection on the symmetry plane, which intersects the ice-cream cone along the central axis, it looks like a triangle represented by thick solid arrows. The central axis of our CME is represented by thick dashed arrow. The inclination of the symmetry axis to the sky plane is γ . Each part of this cone (triangle in projection) has a constant velocity V . The CME with an angular width α is ejected from the solar surface at distance r from the central meridian. Opposite parts of CMEs have velocities, \vec{V}_{x1} and \vec{V}_{x2} , respectively. We note that if the CME originates exactly from the disk center, it will appear at the same time all around the occulting disk. If the source location of CME is slightly shifted ($= r$) with respect to the center of the Sun (as in Fig. 1) then the CME will first appear above the left (eastern) side of the occulting disk and finally above the right (western) side of the occulting disk. In that case the halo CME will be asymmetric with respect to the occulting disk. This asymmetry (the difference between times when CME appears at the opposite limbs) is fundamental for our considerations. By simple inspection we see from Fig 1 that on the left (eastern) side of the occulting disk the CME has to travel a distance $2R - r$ with velocity \vec{V}_{x1} to appear in coronagraph at time T_1 such that

$$T_1 = \frac{(2R - r)}{\vec{V}_{x1}} \quad .$$

Similarly, the CME will appear on the right (western) side of the occulting disk after a time

$$T_2 = \frac{(2R + r)}{\vec{V}_{x2}} \quad .$$

From these equations, we determine the time difference

$$\Delta T = T_2 - T_1 = \frac{(2R + r)}{\vec{V}_{x2}} - \frac{(2R - r)}{\vec{V}_{x1}} \quad . \quad (1)$$

From the geometry of the CME shown in the Fig. 1. we get rest of the necessary equations

$$\cos(\gamma) = \frac{r}{R} \quad , \quad (2)$$

– 4 –

$$\cos(\gamma - \frac{\alpha}{2}) = \frac{Vx1}{V} \quad . \quad (3)$$

$$\cos(180^\circ - \gamma - \frac{\alpha}{2}) = \frac{Vx2}{V} \quad . \quad (4)$$

We have four equations and four parameters to determine r , α , V , and γ . The inputs $Vx1$, $Vx2$ and ΔT need to be obtained from observations. In our considerations we use data from SOHO/LASCO C2 coronagraph with projected radius of occulting disk approximately equal $2R$. To reduce errors we determine the inputs parameters from height-time plots extrapolated to the projected heliocentric distance equal $2R$ also.

2.1. Determination of parameters describing halo CMEs

Obtaining $Vx1$, $Vx2$ and ΔT from LASCO observations is not an easy task because the halo CMEs are typically very faint, and their structure is often very complicated. From LASCO observations we obtained two height-time plots for each halo CME from our sample. The first height-time plot is for that part of the CME which appears as the first above the occulting disk. At the time of the first appearance, each CME arrives at a different height, so we extrapolated the plot to estimate the time ($T1$) when it reaches a heliocentric distance = $2R$ and hence obtain the velocity $Vx1$. The second height-time plot from the opposite limb (where the halo CME appears as last) is used to determine $T2$ and $Vx2$. We illustrate this method using the example of 1999/06/29 CME shown in Fig. 2. In the first panel at the time $T0$ we do not see any new event. In the next panel we see that the CME appears at 07:31 UT in the north-west quadrant of the Sun. From the height-time plot, we get $T1 = 07 : 19$ UT and $Vx1 = 635km/s$. In the next panel, we see that the final part of CME appears in the south-west quadrant of the Sun. From this part we determine $T2 = 07 : 34$ and $Vx2 = 515km/s$. In the fourth panel we can see the full image of the halo CME. The thick solid arrow represents the axis along which the respective parameters are determined. The position angle (PA = angle between the north pole of the Sun and the part of the halo CME where the $Vx1$ is determined) is also indicated. Hence the time difference for this event will be $\Delta T = T2 - T1 = 15min$. Now from equations (1, 2, 3 and 4) describing our CME model we can determine the $V = 698km/s$, width = 112° and parameter $r = 0.15$.

3. Results

The height-time plots were measured for each of the halo CMEs in the LASCO CME catalog and the results are presented in Table 1. The first three columns are from the

SOHO/LASCO catalog (date, time and projected speed from LASCO observations). In the next four columns we have listed the input parameters obtained from LASCO images ($PA, Vx1, Vx2, \Delta T$). Parameters estimated from our cone model (r, γ, α, V) are presented in columns 8,9,10 and 11. Short description of the events is given in column 12. Numbers from the range 0 until 3 describe the quality of a given CME. Numbers from 0-3 describe a very faint CME which can't be measured, a faint CME for which we can measure only two points in a height-time plot, a bright CME and finally a very bright CME, respectively. The letters F, B and B? denote front-sided, back-sided, and probably back-sided halo CME, respectively. If a halo CME is too faint to generate height-time plot at opposite limbs, we could not estimate necessary parameters so we left empty space in our table and put quality 0 in the column 12. Similarly, we could not determine the parameters for the symmetric halo CMEs. This is the case when the asymmetry in velocity is less than 10 km/s or when the time difference is less than 10 minutes. For these cases we put 'Sym' in column 12. In column 13, we have listed the source location of the CME from GOES X-flare onset.

3.1. Properties of the halo CMEs

In Table 1 we have presented all the halo CMEs from August 1996 until the end of 2000. We have to note that not all halo CMEs look identical. We have to consider two types of halo CMEs. First, the classical full halo CMEs which appear to surround the occulting disk very fast in the LASCO/C2 field of view. Generally, they originate from region close to the disk center. Secondly, the wide limb CMEs which surround the entire occulting disk very late, often in the field of view of the LASCO/C3. Sometimes limb events appear as halo due to deflections of pre-existing coronal structures by the fast CME. So we have to be very careful to distinguish between a real halo CME and a limb fast event deflecting coronal material. We were able to determine the respective parameters for 72 CMEs from our sample. For reasons such as complicated or symmetric structures and faintness it was difficult to accomplish necessary measurements for rest of the events from the list. In the three histograms (Fig. 3, Fig. 4, Fig. 5) we present distribution of V , α , and γ . It was noted before, e.g., by Webb et al. (1999) that halo CMEs are much faster and more energetic than typical CMEs. This is also confirmed by our results. The average width of halo CME is approximately equal 120° (more than two times larger than the average value obtained from the SOHO/LASCO catalog (Yashiro et al., 2002)). The most narrow CME has its width equal 40° and the widest one has the cone angle as large as 172° . The average speed of the halo CMEs is 1080km/s (about two times larger than that from SOHO/LASCO catalog). The slowest one had its speed equal to 95km/s while the fastest one had its speed equal to 2590km/s . Fig. 5 shows that the halo CMEs originate close to the sun center (with $\gamma \geq 60^\circ$)

with maximum of distribution around $\gamma = 65^\circ$. We have to remember that we have excluded the symmetric halos, which start exactly from the Sun center. If we include them then the maximum of γ distribution would be shifted to the central meridian. In the Fig. 6 we present the sky plane speeds against corrected (true) velocities. The solid line represents the linear fit to the data points. The inclination of the linear fit suggests that the projection effect increases slightly with the speed of CMEs. It is clear that the projection effect is important and in average the corrected speeds are 20% larger than the velocities measured in the plane of sky.

4. Summary

In this paper we have presented a new method of estimating the crucial parameters determining geoeffectiveness of the halo CMEs. The crucial point of this method is the time difference between the appearances of the halo at two opposite position angles. We applied this method to all the halo CMEs listed in the SOHO/LASCO catalog until the end of 2000. We were able to determine the true velocity, width and source location for 72 CMEs from our sample. Unfortunately, 58 events were either symmetric or too faint to measure. These results suggest that the halo CMEs represent a special class of CMEs which are very wide and fast. Such fast and wide CMEs are known to be associated with electron and proton acceleration by driving fast mode MHD shocks (e.g., Cane et al. 1987, Gopalswamy et al., 2001; 2002a). We point out that the simple method has several shortcomings: (i) CMEs may be accelerating, moving with constant speed or decelerating at the beginning phase of propagation. This means that the constant velocity assumption may be invalid. (ii) CMEs may expand in addition to radial motion. Then the measured sky-plane speed is a sum of the expansion speed and the projected radial speed. This would also imply that the CMEs may not be a rigid cone as we had assumed (Gopalswamy et al. 2002b) (iii) The cone symmetry also may not hold. Many halo CMEs do not emerge over opposite limbs along a symmetrical 180 degrees, they structure is often very complicated. Unfortunately, beautiful events similar to the one presented in the Fig. 2 are sporadic. It is very difficult to estimate how reliable our basic assumptions (CMEs have constant velocities, constant angular width, and are symmetric) are for a given CME. Each of these assumptions may be true for most CMEs but not necessarily for a particular CME. Nevertheless, here is no available data to modify the model. For our consideration we chose only bright halo CMEs with large difference in appearance time above opposite limbs. There is still a possibility that the determined parameters for a particular halo CME (for CMEs which completely breaks our basic assumptions) may be wrong. The 'exotic' events, if they exist in our sample at all, should not affect our results. All these limits can be overcome by stereoscopic observations.

Unfortunately, at the present time they are not available yet. It is necessary to improve the model to get a better fit to the observations. The first step would be to include acceleration and expansion of CMEs. We have to note that it may be surprising that the average corrected speeds are only 20 percent greater than the skyplane speeds. But we have to remember that halo CMEs originating close to the Sun center, subjected to the largest projection effects, are not included in our results. They are symmetric in LASCO observations and cannot be considered using our method.

This paper was done during work of Grzegorz Michalek at Center for Solar and Space Weather, Catholic University of America in Washington.

In this paper we used data from SOHO/LASCO CME catalog. This CME catalog is generated and maintained by the Center for Solar Physics and Space Weather, The Catholic University of America in cooperation with the Naval Research Laboratory and NASA. SOHO is a project of international cooperation between ESA and NASA.

Work done by Grzegorz Michalek was partly supported by *Komitet Badań Naukowych* through the grant PB 258/P03/99/17.

REFERENCES

- Cane, H.V., et al., 1987, *J. Geophys. Res.*, 92, 9869
- Fisher, R.R., Munro, R.H., 1984, *ApJ*, 280, 873
- Gopalswamy, N., et al. 2000a, *Geophys. Res. Lett.*, 27, 145
- Gopalswamy, N., et al., 2000b, et al., *Geophys. Res. Lett.*, 27, 1427
- Gopalswamy, N., et al. 2001, *J. Geophys. Res.*, 106, 292907
- Gopalswamy, N., 2002a, *ApJ*, 572, L103
- Gopalswamy, N., 2002b, *Cospar Colloquia Series*, 12, 39
- Howard R.A., et al. 1982, *ApJ*, 263, L101
- Leblanc, Y., Dulk, G.A., 2001, *J. Geophys. Res.*, 106, 25301
- Sheeley, N.R., Jr., Walters, J.H., Wang, Y.-M., Howard, R.A. 1999, *J. Geophys. Res.*, 104, 24739
- St. Cyr, O.C., et al. 2000, *J. Geophys. Res.*, 105, 18169
- Webb, D.F., et al. 1997, *J. Geophys. Res.*, 102, 24161
- Webb, D.F., et al. 1999, *BAAS*, Vol. 31, p. 853
- Yashiro, S., et al. 2002, *BAAS*, Vol. 34(No.2), abstract 37.04
- Zhao, X-P., et al. 2002, *J. Geophys. Res.*, in press

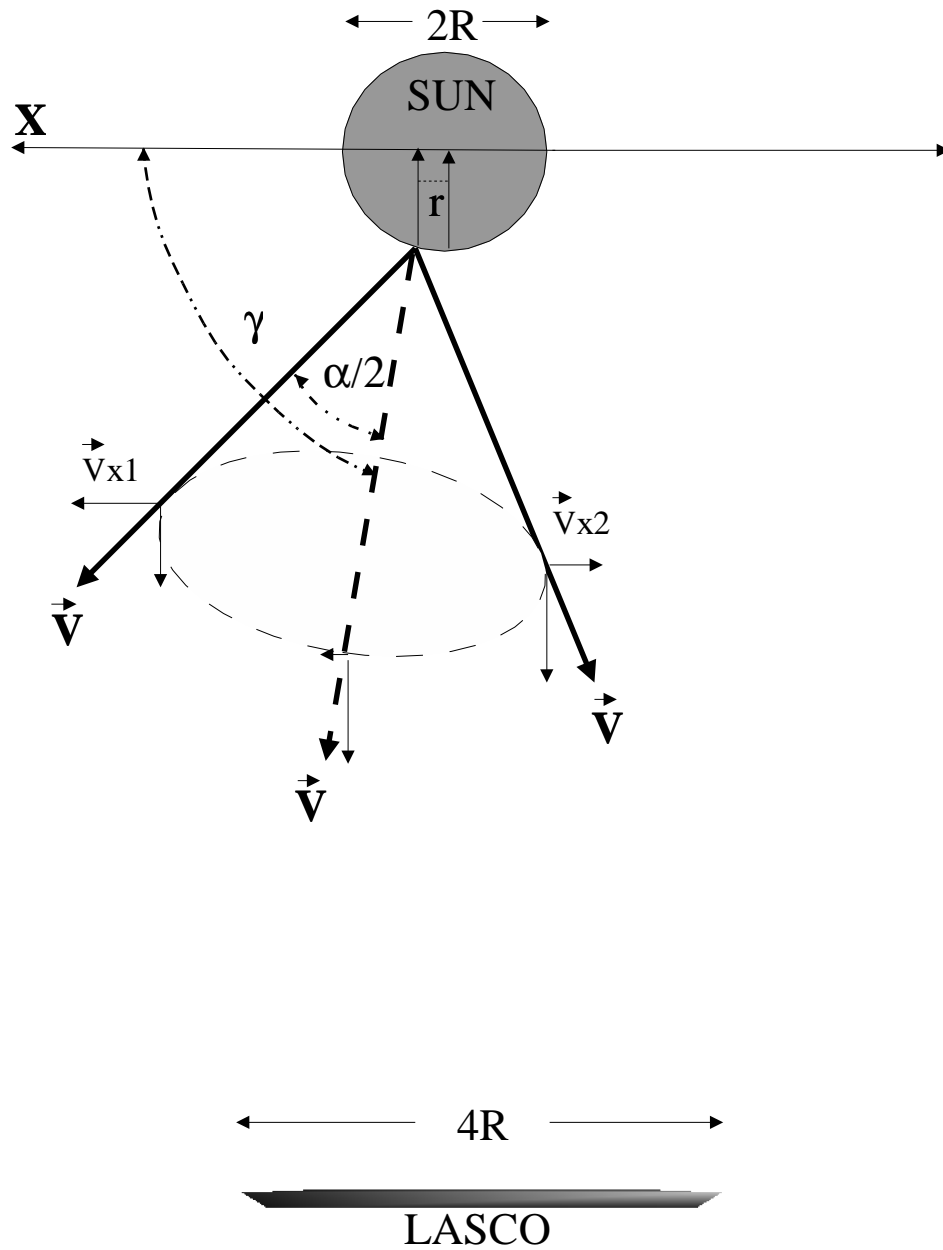


Fig. 1.— The schematic picture presenting our cone model of the halo CME. In the bottom of the picture we see the occulting disk of the LASCO/C2 coronagraph. It should be note that this is only a schematic picture without a real scale.

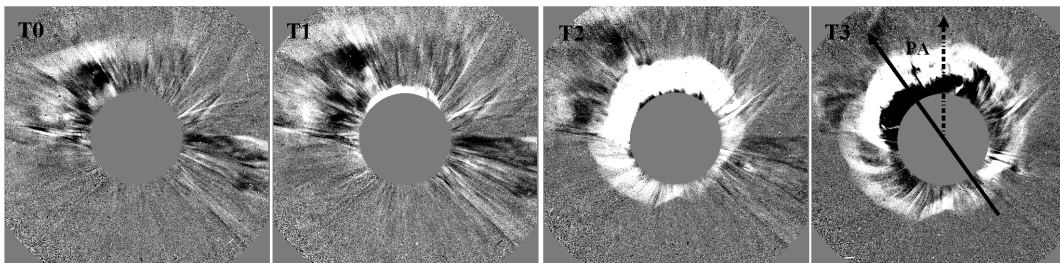


Fig. 2.— In the successive panels we present expansion of 1999/06/29 halo CME monitored by the LASCO/C2 coronagraph. In the last panel, the thick solid arrows present the axis along which $Vx1$ and $Vx2$ are determined. The position angle (PA = angle between north pole of the Sun and part of the halo CME where the $Vx1$ is determined) is indicated also.

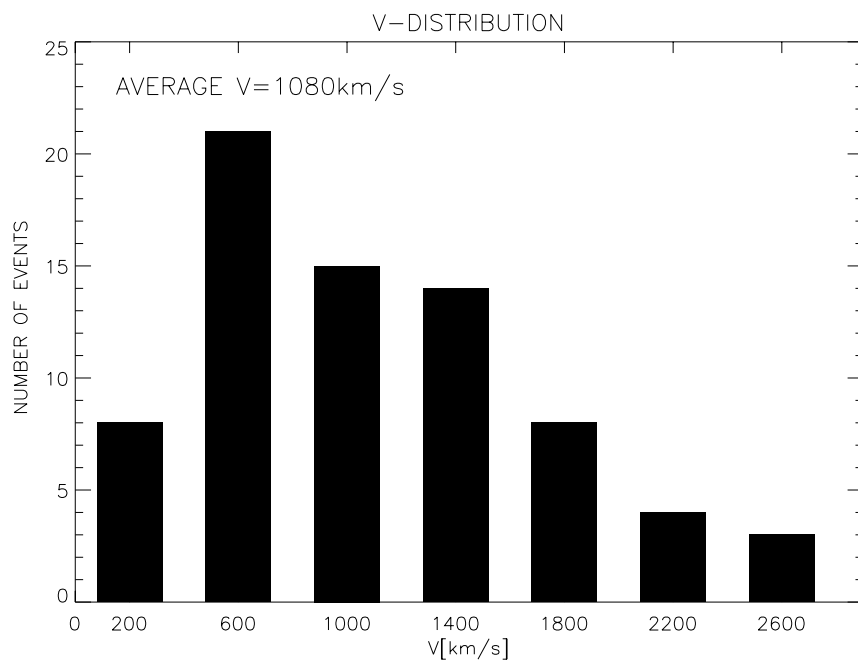


Fig. 3.— The histogram showing distribution of V for the halo CMEs.

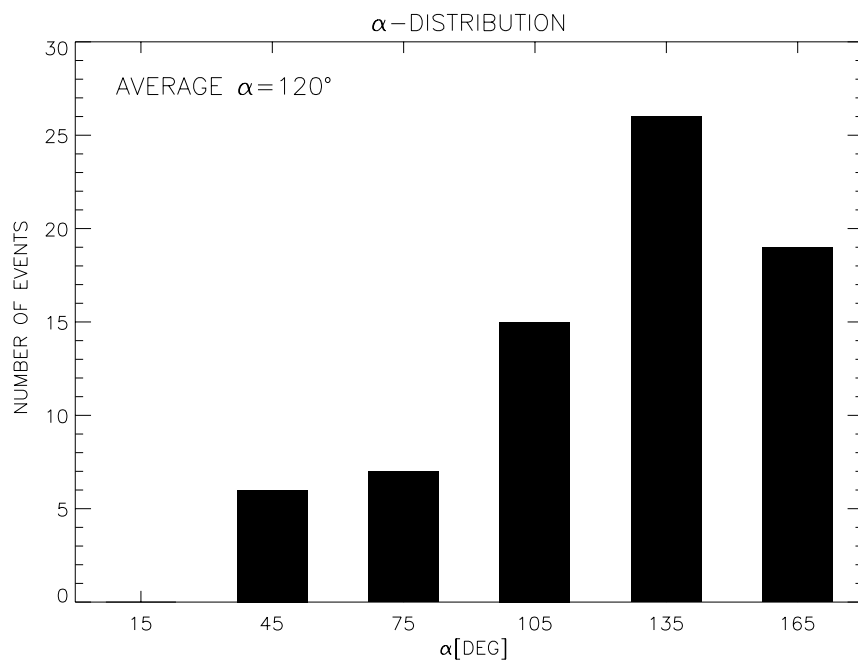


Fig. 4.— The histogram showing distribution of α for the halo CMEs.

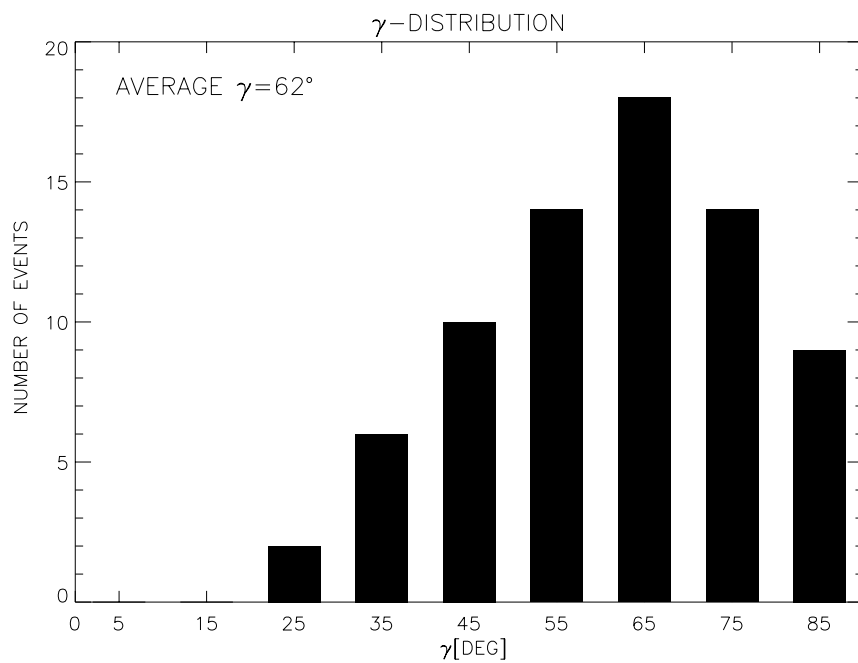


Fig. 5.— The histogram showing distribution of γ for the halo CMEs.

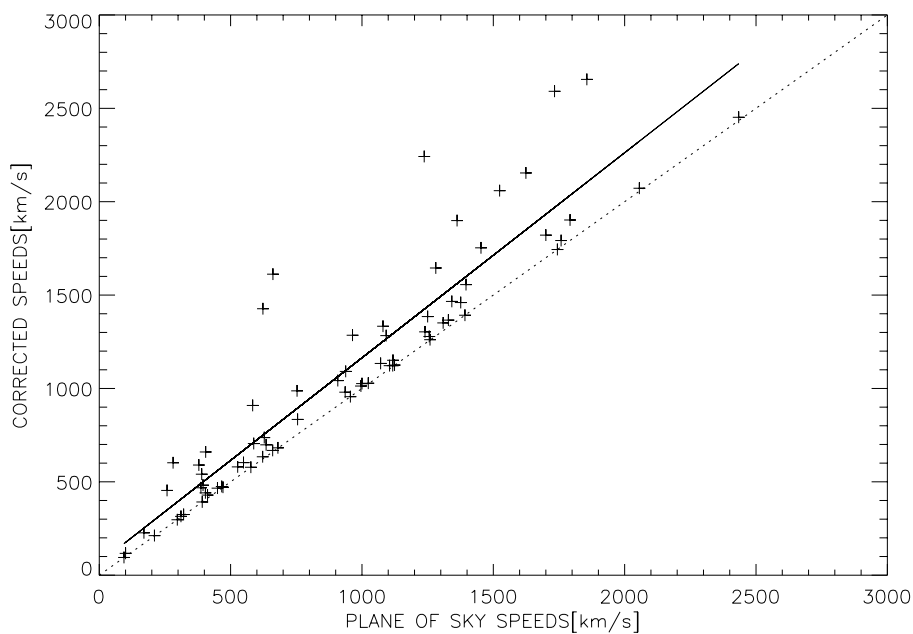


Fig. 6.— The plane of the sky speeds versus the corrected (real) speeds. The solid line shows the linear fit to data

Table 1. List of halo CMEs.

DATA	TIME	SPEED $\frac{km}{s}$	PA Deg	Vx1 $\frac{km}{s}$	Vx2 $\frac{km}{s}$	ΔT Min	r $\frac{1}{R_{\odot}}$	γ Deg	α Deg	V $\frac{km}{s}$	Char	Flare
1996/08/16	14:14:06	364	96	405	220	62	0.17	80	59	660	1.0,B?	—
1996/11/07	23:20:05	497	114	412	361	18	0.16	80	133	429	1.0,B?	—
1996/12/02	15:35:05	538	270	392	232	79	0.47	61	128	392	1.5,B?	—
1997/01/06	15:10:42	136	182	100	85	75	0.13	82	105	117	0.5,F	S20W03
1997/02/07	00:30:05	490	260	297	160	140	0.51	58	121	297	1.5,F	S20W04
1997/04/07	14:27:44	875	126	956	551	23	0.42	65	139	954	2.0,F	S30E19
1997/05/12	06:30:09	464	—	—	—	—	—	—	—	—	Sym	N21W08
1997/07/30	04:45:47	104	276	94	85	81	0.25	75	146	95	1.0,B	—
1997/08/30	01:30:35	405	65	397	163	103	0.21	78	56	590	1.0,F	N30E17
1997/09/28	01:08:33	359	66	210	118	169	0.53	57	131	212	3.0,B	—
1997/10/21	18:03:45	523	30	527	356	35	0.24	75	103	580	1.0,F	N20E12
1997/10/23	11:26:50	503	—	—	—	—	—	—	—	—	0.0,B	—
1997/11/04	06:10:05	755	—	—	—	—	—	—	—	—	Sym	S14W33
1997/11/06	12:10:41	1556	261	1524	765	34	0.82	34	153	2059	1.5,F	S18W63
1997/11/17	08:27:05	611	—	—	—	—	—	—	—	—	Sym	—
1997/12/18	23:47:31	417	68	321	270	40	0.36	68	158	325	2.5,B	—
1998/01/02	23:28:20	438	258	281	142	197	0.93	20	165	602	2.0,B?	—
1998/01/17	04:09:20	350	—	—	—	—	—	—	—	—	0.0,B	—
1998/01/21	06:37:25	361	176	387	265	80	0.71	44	159	468	0.5,F	S57E19
1998/01/25	15:26:34	693	36	471	216	98	0.50	60	114	471	1.0,F	N24E27
1998/03/29	03:48:00	1794	—	—	—	—	—	—	—	—	0.0,B?	—
1998/03/31	06:12:02	1992	167	1733	502	41	0.26	74	53	2591	3.0,B?	—
1998/04/23	06:55:20	1618	113	1744	945	21	0.51	59	126	1744	3.0,F	—
1998/04/27	08:56:06	1434	—	—	—	—	—	—	—	—	0.0,F	S16E50
1998/04/29	16:58:54	1374	16	1071	794	17	0.26	74	111	1134	2.0,F	S17E20
1998/05/01	23:40:09	585	142	623	367	31	0.1	84	40	1427	2.0,F	S18W05
1998/05/02	05:31:56	542	143	661	426	23	0.1	85	39	1612	2.0,F	S20W17
1998/05/02	14:06:12	938	—	—	—	—	—	—	—	—	Sym	S15W15
1998/06/04	02:04:45	1802	—	—	—	—	—	—	—	—	0.0,B	—
1998/06/05	12:01:53	320	223	170	109	215	0.78	39	159	227	1.0,F	S23E43
1998/06/07	09:32:08	794	114	1117	834	17	0.4	66	143	1122	2.0,B	—
1998/06/20	18:20:37	964	153	964	481	54	0.8	35	153	1285	2.0,B?	—
1998/10/24	02:18:05	452	116	404	377	32	0.46	62	172	441	1.5,B?	—
1998/11/04	04:54:07	527	0.0	390	158	114	0.25	75	62	541	1.5,F	N17W01
1998/11/05	02:24:56	577	288	395	267	42	0.18	79	88	482	1.0,F	N19W10
1998/11/05	20:58:59	1124	305	1092	378	55	0.35	69	75	1283	3.0,F	N22W18
1998/11/24	02:30:05	1744	224	1856	628	43	0.88	27	153	2655	3.0,F	S30W81
1998/11/26	03:42:05	488	—	—	—	—	—	—	—	—	0.0	—
1998/12/18	18:21:50	1745	40	1758	532	50	0.68	47	120	1792	2.0,F	N19E64
1999/04/04	04:30:07	1178	—	—	—	—	—	—	—	—	0.0,F	N18E72
1999/04/24	13:31:15	1495	307	1259	502	45	0.52	58	110	1261	2.0,B	—
1999/05/03	06:06:05	1584	50	1392	345	61	0.61	51	110	1369	2.0,F	N15E32
1999/05/10	05:50:05	920	80	1080	513	33	0.27	74	76	1333	1.5,F	N16E19
1999/05/27	11:06:05	1691	311	1700	623	42	0.71	44	130	1821	1.5,B	—
1999/06/01	19:37:35	1772	351	1792	662	32	0.40	65	88	1902	1.5,B	—
1999/06/04	00:50:06	803	8	936	475	38	0.37	68	101	980	1.5,B?	—
1999/06/08	21:50:05	726	10	755	690	19	0.49	60	170	834	1.5,F	N30E03
1999/06/12	21:26:08	465	—	—	—	—	—	—	—	—	Sym	N22E37
1999/06/22	18:54:05	1133	—	—	—	—	—	—	—	—	0.0,F	N22E37
1999/06/23	06:06:05	450	—	—	—	—	—	—	—	—	Sym	S10E71
1999/06/23	07:31:24	1006	—	—	—	—	—	—	—	—	Sym	S12E78
1999/06/24	13:31:24	975	—	—	—	—	—	—	—	—	0.0,F	N29E13
1999/06/26	07:31:25	558	0	584	419	21	0.11	83	67	909	1.0,F	N25E00
1999/06/28	12:06:07	560	364	549	297	77	0.67	47	143	603	1.0,F	S27E55
1999/06/28	21:30:08	1083	—	—	—	—	—	—	—	—	0.0,F	S25E49
1999/06/29	05:54:06	589	—	—	—	—	—	—	—	—	0.0	—
1999/06/29	07:31:26	634	10	635	515	15	0.15	81	112	698	2.0,F	N18E07
1999/06/29	18:54:07	438	—	—	—	—	—	—	—	—	0.0,F	S14E01
1999/06/30	04:30:05	1049	—	—	—	—	—	—	—	—	0.0	—
1999/06/30	11:54:07	627	193	588	424	23	0.16	80	92	705	1.0,F	S15E00
1999/06/30	13:31:25	514	—	—	—	—	—	—	—	—	0.0	—
1999/07/06	17:06:05	899	350	1000	489	39	0.41	65	105	1026	1.0,B	—
1999/07/19	03:06:05	509	—	—	—	—	—	—	—	—	0.0,F	N15W13
1999/07/25	13:31:21	1389	306	1342	348	82	0.76	40	127	1466	2.0,F	N29W81
1999/07/28	05:30:05	457	—	—	—	—	—	—	—	—	0.0,F	S15E00
1999/07/28	09:06:05	456	—	—	—	—	—	—	—	—	0.0,F	S15E04

